

# Chapter 1

## Triboelectrification

The massive development of the world electronic technology follows a general trend of miniaturization, portability and functionality. The development of computers is a typical example of miniaturization, from the vacuum tube based huge-size machine, to solid state metal–oxide–semiconductor field-effect transistor (MOSFET) based main frame computer and later laptop computer. The tremendous increase of popularity of handheld cell phones is a typical example of portable/mobile electronics. The next few decades will be about building functionality on existing electronics, which inevitably involves developing a range of sensors including but not limited to navigation, motion, chemical, biological and gas sensors. The near future development is about electronics that are much smaller than the size of a cell phone, so that each person on average can have at least dozens to hundreds of such small electronics. Such small size electronics operates at ultralow power consumption, making it possible to be powered by the energy harvested from our living environment [1]. It will become impractical if sensor networks have to be powered entirely by batteries because of the huge number of devices, large scope of distribution, and difficulty to track and recycle to minimize environmental impact and possibly health hazardous. Therefore, power sources are desperately needed for independent and continuous operations of such small electronics, which could be used widely for ultrasensitive chemical and bimolecular sensors, nanorobotics, micro-electromechanical systems, remote and mobile environmental sensors, homeland security and even portable/wearable personal electronics.

New technologies that can harvest energy from the environment as sustainable self-sufficient micro/nano-power sources are newly emerging field of nano energy, which is about the applications of nanomaterials and nanotechnology for harvesting energy for powering micro/nano-systems. In the last decade, we have been developing nanogenerators (NGs) for building self-powered systems and as active sensors [2]. We have mainly utilized two physics effects for harvesting small-magnitude mechanical energies: piezoelectric effect and triboelectric effect. A basic introduction about piezoelectric NG has been given in a recent book [2] and

a few review articles [3, 4]. The objective of this book is to give a systematic and comprehensive introduction about triboelectric nanogenerator (TENG) from theory to experiments, from fundamental operation modes to technological application, from single devices to system integration, both as a new energy technology and as self-powered active sensors.

## 1.1 Nano Energy and Mega Energy

In general, energy usually means the power required to run a factory, a city or a country. This is generally referred to as mega energy, which is measured in the scale of Giga Watt or Mega Watt. General characteristics of a technology for macro-scale energy are the total power output, stability, conversion efficiency and cost. In many cases, cost is the most important measure, such as for solar cell (Fig. 1.1).

On the other hands, with the tremendous increase in the number of portable electronics, developing energy storage related technologies is vitally important because most of which are run by batteries. Although the power consumption of each is rather small, the total number of devices is extremely huge. Over three billion people around the world have cell phones. With the implementation of sensor networks around the globe, a gigantic number of sensors will be distributed worldwide; powering of such a horrendous network consisting of trillions of sensors would be impossible using batteries, because one has to find the location, replace batteries and

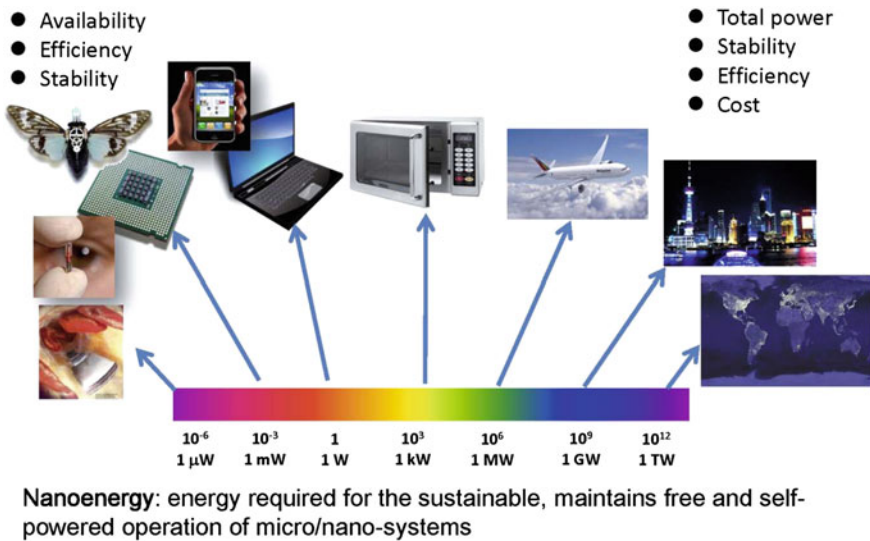


**Fig. 1.1** Magnitude of power and its corresponding applications. Macro-scale energy is for powering a city and even a country, the nano-scale energy is to power tiny small electronics, both of such applications are measured by different characteristics. Reproduced with permission from Wiley [5]

inspect the proper operation of batteries from time to time. Energy harvesting from the environment in which the sensor is employed is a possible solution. This is the field of nano energy, which is the power for sustainable, maintains free and self-powered operation of micro/nano-systems [5]. The general characteristics for nano energy power sources are the availability, efficiency and stability (Fig. 1.1). In a case that a device is used under the light, the use of solar energy would be a natural choice. In a case of a device is used near an engine possibly in dark, harvesting mechanical vibration energy would be the best choice. As for biological application, harvesting deformation energy from muscle stretching would be a good approach. Although we may have a super high efficient solar cell, the condition under which the device will work may have little light, the high efficient solar cell is not the choice for this device. Therefore, the type of energy to be harvested depends on the working environment of the device. This is what we mean by the availability of the energy source for a particular application. The stability of the energy source is also important because it guarantee the long-term operation of the device. Take solar cell as an example, it has strong dependence on the day or night, weather or even season. This is the reason that we have been developing technologies for converting mechanical energy into electricity for self-powered sensors.

## 1.2 Triboelectric Effect

The triboelectric effect is a contact induced electrification in which a material becomes electrically charged after it is contacted with a different material through friction. Triboelectric effect is a general cause of every day's electrostatics. The signed of the charges to be carried by a material depends on its relative polarity in comparison to the material to which it will contact.

Triboelectric effect is probably the only a few effects that have been known for thousands of years. Although this is one of the most frequently experienced effect that each and every one of us inevitably uses every day, the mechanism behind triboelectrification is still being studied possibly with debate [6, 7]. It is generally believed that after two different materials coming into contact, a chemical bond is formed between some parts of the two surfaces, called adhesion, and charges move from one material to the other to equalize their electrochemical potential. The transferred charges can be electrons or may be ions/molecules. When separated, some of the bonded atoms have a tendency to keep extra electrons, and some a tendency to give them away, possibly producing triboelectric charges on surfaces.

Materials that usually have strong triboelectrification effect are likely less conductive or insulators, thus, they usually capture the transferred charges and retain them for an extended period of time, building up the electrostatic charges, which are usually attributed to as negative effect in our daily life and technology developments. We can use the following examples to illustrate the damages that can be caused by triboelectrification. Aircraft flying will develop static charges from air friction on the airframe, which will interfere with radio frequency communication. Electrostatic

charges are an important concern for safety, due to the fact that it can cause explosion and ignite flammable vapors. Carts/cars that may carry volatile liquids, flammable gasses, or explosive chemicals have to be discharged properly to avoid fire. Some electronic devices, most notably complementary metal-oxide semiconductor (CMOS) integrated circuits and MOSFET transistors, can be accidentally destroyed by high-voltage static discharge that may be carried by gloves. Therefore, triboelectrification is mostly taken as a negative effect in our daily life, industrial manufacturing and transportation. Therefore, by surprise, although triboelectrification is known for thousands of years, it has not been used for many positive applications. It is until recently that triboelectric effect has been widely used for converting mechanical energy into electricity and as self-powered active mechanical sensors.

### 1.3 Quantification of Triboelectrification

Although the triboelectrification effect is known for thousands of years, a fundamental understanding about it is rather limited. Research has been conducted to characterize the triboelectrification process using various methods such as rolling sphere tool-collecting induced charges from rolling spheres on top of dielectric disk [8, 9], and using atomic force microscopy (AFM) to measure surface electrostatic force or potential on surfaces contacted by micro-patterned materials [10–12]. However, these methods either lack an accurate control of the electrification process and/or cannot directly reveal the triboelectric interface, thus hardly achieving a quantitative understanding about the in situ triboelectric process.

We have demonstrated an in situ method to quantitatively characterize the triboelectrification at nano-scale via a combination of contact-mode AFM and scanning Kelvin probe microscopy (SKPM) [13]. Benefited from the capability of controlled charge transferring and in situ measurement, AFM can be used to investigate the triboelectric charge transfer at surfaces. As a model system, a  $\text{SiO}_2$  thin film was rubbed for multiple cycles at the same area with constant contact force. The corresponding SKPM images after each friction cycle are shown in Fig. 1.2a and the extracted potential profiles are presented in Fig. 1.2b. Within eight cycles of friction, the magnitude of the potential increased from 0.1 to 0.7 V at a slowing rate. As shown in Fig. 1.2c, there is a clear trend for the surface charge accumulation and saturation process. By quantitatively fitting the experimental data, surface charge density before triboelectric process is  $\sigma_0 = (-12 \pm 3) \mu\text{C}/\text{m}^2$ , and saturation charge density after infinite numbers of cycles of friction is  $\sigma_\infty = (-150 \pm 8) \mu\text{C}/\text{m}^2$ . The electric field at the vicinity of the surface is  $\sim 1.7 \times 10^7 \text{ V/m}$ , which can easily generate a high voltage. The contact induced charge transfer is the experimental base of our TENG.

The charges to be delivered to the surface of material can be manipulated by applying a bias at the tip. Here we present the effect of an extrinsically applied electric field on contact electrification between metals and dielectric films [14]. Figure 1.3a schematically displays the charge transfer between a metal and a

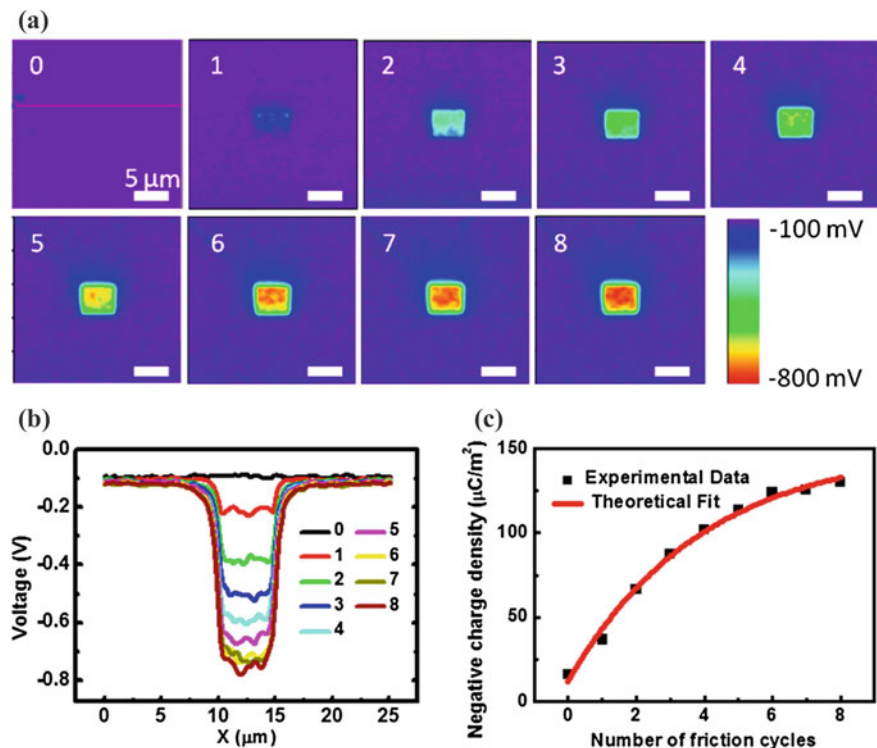


**Fig. 1.2** Triboelectric charge accumulation on the SiO<sub>2</sub> surface with the increase of the number of repeated rubbing at the same area. **a** Series of surface potential images taken in the same area from intact status to the one after 8th rubbing cycles, and **b** their corresponding potential profiles. **c** Derived surface charge density as a function of the number of friction cycles, and our fit based on charge accumulation theory. Reproduced with permission from American Chemical Society [13]

dielectric layer in contact electrification. When the top electrode contacts the dielectric layer, according to the electron transfer mechanism [15, 16], electrons will transfer from one to the other due to the difference in the effective work functions of two materials. Subsequently, the transferred contact electric charges can also induce opposite charges in the two metal electrodes due to electrostatic induction. Although the equivalent band gap in dielectric materials are large (usually larger than 8 V), it usually has surface states within the bandgap that can accommodate electrons [14]. Here we utilized the energy band diagrams to illustrate the case of a triboelectrically negative dielectric material (as compared to the metal). Accordingly, the highest filled surface energy states of the dielectric material is below the Fermi level of the metal, as illustrated in Fig. 1.3b. When the two materials are in contact, electrons in the metal will flow from the top metal electrode onto the dielectric surface to fill up the surface states as high as the metal's Fermi level (Fig. 1.3c). When two materials are separated from each other, an electric field is built up due to the transferred charge on the dielectric surface and image charges on the metal side, as depicted in Fig. 1.3d. The strength of the

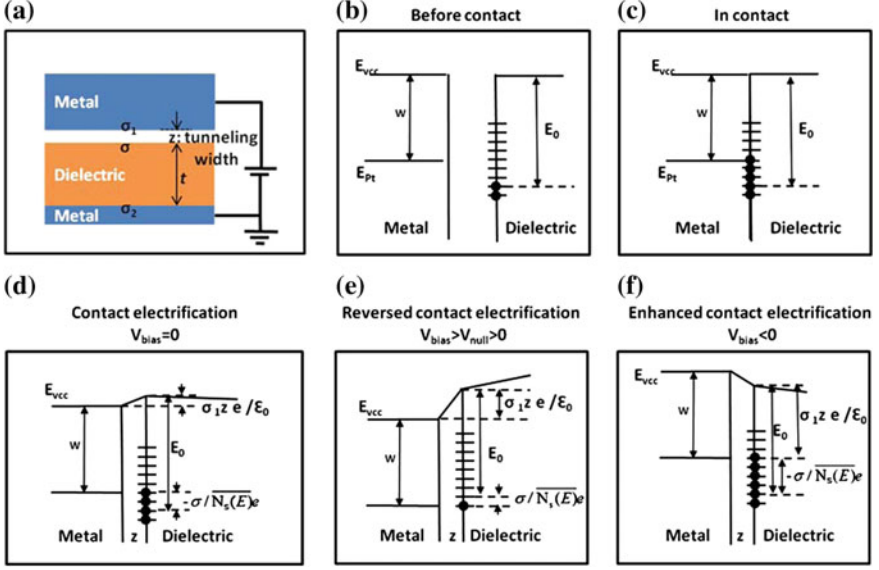


**Fig. 1.3** **a** Illustration of the contact electrification process with a tunneling width  $z$ , the charge transferred to the dielectric surface with a density of  $\sigma$ , induced charge density  $\sigma_1$  and  $\sigma_2$ . **b–f** Energy band diagrams for the metal and dielectric materials in the situations of pre-contact (**b**), in contact with no bias (**c**), in separation equilibrium with no (**d**), positive (**e**) and negative (**f**) bias. Reproduced with permission from American Chemical Society [14]

electric field is proportional to the induced charge density  $\sigma_1$  in the metal side. Due to this locally built-up electric potential, a portion of the charges on the dielectric surface can flow back to the metal. The potential difference is determined by the separation distance and electric field strength. At the same time, the separation process also creates an energy barrier between two surfaces that hinders the back-flow of electrons. For simplicity, we assign a critical tunneling distance  $z$ , and assume that below  $z$  the electrons can flow freely between two surfaces to maintain a constant Fermi level and above  $z$  the barrier is large enough to prevent any tunneling. For a parallel-plates model, at the distance  $z$ , the dielectric surface charge  $\sigma$  induces  $\sigma_1$  on the top metal and  $\sigma_2$  on the bottom metal, which should satisfy

$$\sigma + \sigma_1 + \sigma_2 = 0 \quad (1.1)$$

Due to built-in electric field  $\sigma_1/\epsilon_0$ , the vacuum energy level between the metal and the dielectric surface changes by  $\Delta E_{vcc}$ :

$$\Delta E_{vcc} = \sigma_1 z e / \epsilon_0 \quad (1.2)$$

where  $e$  is the elementary charge.

When the system is in equilibrium, the dielectric surface state will be filled up as high as the Fermi energy level in the metal. If we assume that the surface density of states is  $N_s(E)$  and the range of filled surface states is  $\Delta E_s$ , we have

$$\sigma = -e \int_{E_0}^{E_0 + \Delta E_s} N_s(E) dE \quad (1.3)$$

Here, we use the averaged surface density of states as defined below,

$$\overline{N_s(E)} = \frac{\int_{E_0}^{E_0 + \Delta E_s} N_s(E) dE}{\Delta E_s} \quad (1.4)$$

Therefore, the range of filled surface states  $\Delta E_s$  can be described as

$$\Delta E_s = -\sigma / \overline{N_s(E)} e \quad (1.5)$$

Combining Eqs. (1.2) and (1.5), we have,

$$E_0 - W = \Delta E_{vcc} + \Delta E_s = \sigma_1 z e / \epsilon_0 - \sigma / \overline{N_s(E)} e \quad (1.6)$$

An external potential applied between the top and bottom (electrode underneath the dielectric film) metals will change the relative energy band height, which modulates the charge transfer accordingly. A positive bias applied to the top metal can lower its Fermi energy level, thus reducing the number of electrons transferred from the metal to the dielectric. At certain bias, the Fermi energy level will be as low as the highest filled surface states in the dielectric material. As a result, no charge will transfer between the metal and the dielectric surface, suggesting the contact electrification will be nullified. When the bias is more positive than the nullified bias, electrons will flow in a reversed way from the dielectric to the metal, leaving dielectric surface positively charged, as illustrated in Fig. 1.3e. On the contrary, a negative bias to the metal can raise its Fermi energy level, driving more electrons flow to the dielectric surface to fill up higher surface energy states, resulting in the dielectric surface to be more negatively charged (Fig. 1.3f). Under the parallel-plate assumption, the bias  $V$  between two metal electrodes can be written using Poisson equation as:

$$V = \frac{\sigma_1}{\epsilon_0} z - \frac{\sigma_2}{\epsilon \epsilon_0} t \quad (1.7)$$

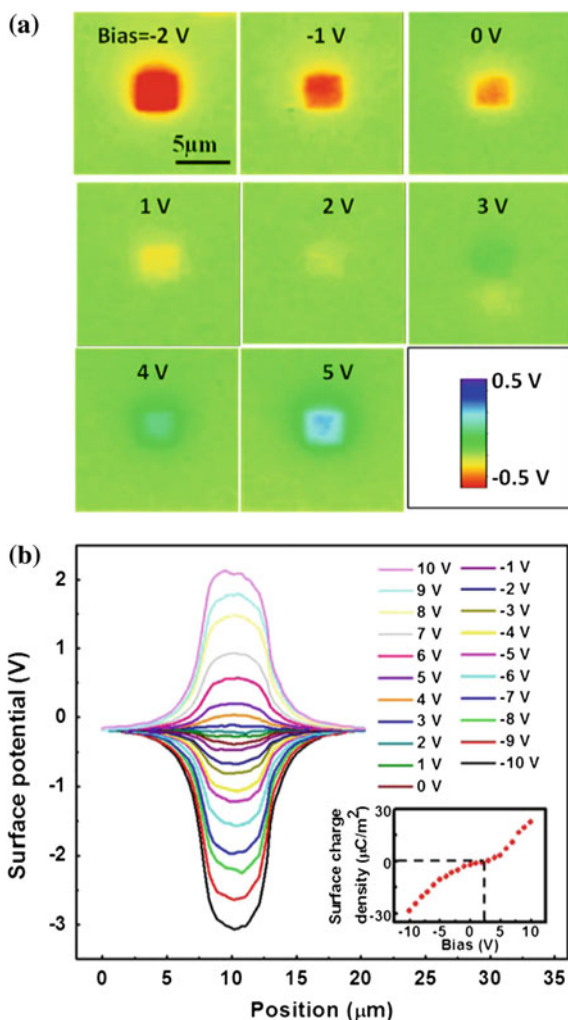
Combining Eqs. (1.1), (1.6) and (1.7), we can derive the surface charge density on the dielectric surface  $\sigma$  as [14]:

$$\sigma = \frac{V + \frac{(W-E_0)}{e} (1 + t/\epsilon z)}{t/\epsilon \epsilon_0 + \frac{1}{\overline{N_s(E)} e^2} (1 + t/\epsilon z)} \quad (1.8)$$

This equation provides a guideline on how the external electric field quantitatively modulates the contact electrification.

From Eq. (1.8), the transferred charge density  $\sigma$  should change with the externally applied bias  $V$ . To quantify the electric field influence, fresh areas of a Parylene film (2  $\mu\text{m}$  in thickness) were rubbed with different bias from  $-10$  to  $10$  V and then measured in the SKPM mode. Figure 1.4a displays the surface potential distribution in the areas that were rubbed with biases from  $-2$  to  $5$  V: a negative bias can enhance the negative charge density; a positive bias of  $2$  V almost nullified

**Fig. 1.4** **a** Surface potential distributions of the Parylene film including the areas that were rubbed by Pt coated AFM tip at different bias from  $-2$  to  $5$  V. **b** Cross section profiles of the surface potential of the Parylene film rubbed with bias from  $-10$  to  $10$  V. The *inset* is the calculated surface charge density as a function of bias. With a bias of about  $2.5$  V, the surface charge density is zero, indicating the contact electrification is completely canceled out by the applied bias. Reproduced with permission from American Chemical Society [14]





the charges; a bias of higher than 2 V brought positive charges to the rubbed surface. A cross section profile of the surface potential distribution of each experiment was plotted in Fig. 1.4b. The surface potential of the rubbed area is adjusted monotonically by the applied bias, where the positive bias brings the surface potential to be more positive, and the negative bias exhibits the opposite effect. The corresponding surface charge density calculated from the surface potential profile is plotted as a function of the applied bias during the rubbing process in the inset of Fig. 1.4b. It can be seen that the surface charge density increases with increasing the applied external bias with a nonlinear characteristic, which is associated with the different energy state densities in the middle of band gap and closer to the conduction/valence band.

## 1.4 Materials for Triboelectrification

Almost any materials we know have triboelectrification effect, from metal, to polymer, to silk and to wood, almost everything. All of these materials can be candidates for fabricating TENGs, so that the materials choices for TENG are huge. However, the ability of a material for gaining/losing electron depends on its polarity. John Carl Wilcke published the first triboelectric series in a 1757 on static charges [16, 17]. Table 1.1 gives such a series for some conventional materials. A material towards the bottom of the series, when touched to a material near the top of the series, will attain a more negative charge. The further away two materials are from each other on the series, the greater the charge transferred. Recently, using the contact between a solid and liquid metal, such as Hg, a methodology has been established to quantitatively measure the surface charge density as a result of triboelectrification (see Sect. 7.4).

Beside the choice of the materials in the triboelectric series, the morphologies of the surfaces can be modified by physical techniques with the creation of pyramids-, square- or hemisphere-based micro- or nano-patterns, which are effective for enhancing the contact area and possibly the triboelectrification. The surfaces of the materials can be functionalized chemically using various molecules, nanotubes, nanowires or nanoparticles, in order to enhance the triboelectrification effect. Surface functionalization can largely change the surface potential. The introduction of nanostructures on the surfaces can change the local contact characteristics. The contact materials can be made of composites, such embedding nanoparticles in polymer matrix. This not only changes the surface electrification, but also the permittivity of the materials so that they can be effective for electrostatic induction.

**Table 1.1** Triboelectric series for some commonly materials following a tendency of easy losing electrons (positive) to gaining electrons (negative) [7]

<div>Positive</div> <div></div>	Polyformaldehyde 1.3-1.4	(continued)	<div></div> <div>Negative</div>
	Etylcellulose	Polyester (Dacron)	
	Polyamide 11	Polyisobutylene	
	Polyamide 6-6	Polyurethane flexible sponge	
	Melamine formol	Polyethylene Terephthalate	
	Wool, knitted	Polyvinyl butyral	
	Silk, woven	Polychlorobutadiene	
	Aluminum	Natural rubber	
	paper	Polyacrilonitrile	
	Cotton, woven	Acrylonitrile-vinyl chloride	
	Steel	Polybisphenol carbonate	
	Wood	Polychloroether	
	Hard rubber	Polyvinylidene chloride (Saran)	
	Nickel, copper	Polystyrene	
	Sulfur	Polyethylene	
	Brass, silver	Polypropylene	
	Acetate, Rayon	Polyimide (Kapton)	
	Polymethyl methacrylate (Lucite)	Polyvinyl Chloride (PVC)	
	Polyvinyl alcohol	Polydimethylsiloxane (PDMS)	
	(continued)	Polytetrafluoroethylene (Teflon)	

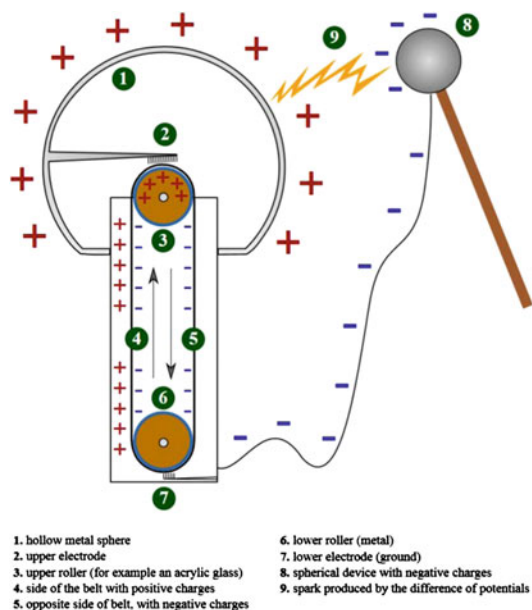
(continued)

Table 1.1 (continued)

<div>Positive</div> <div></div>	Aniline-formol resin	Polyvinyl alcohol	<div></div> <div>Negative</div>
	Polyformaldehyde 1.3-1.4	Polyester (Dacron) (PET)	
	Etylcellulose	Polyisobutylene	
	Polyamide 11	Polyuretane flexible sponge	
	Polyamide 6-6	Polyethylene terephthalate	
	Melanime formol	Polyvinyl butyral	
	Wool, knitted	Formo-phenolique, hardened	
	Silk, woven	Polychlorobutadiene	
	Polyethylene glycol succinate	Butadiene-acrylonitrile copolymer	
	Cellulose	Nature rubber	
	Cellulose acetate	Polyacrilonitrile	
	Polyethylene glycol adipate	Acrylonitrile-vinyl chloride	
	Polydiallyl phthalate	Polybisphenol carbonate	
	Cellulose (regenerated) sponge	Polychloroether	
	Cotton, woven	Polyvinylidine chloride (Saran)	
	Polyurethane elastomer	Poly(2,6-dimethyl polyphenyleneoxide)	
	Styrene-acrylonitrile copolymer	Polystyrene	
	Styrene-butadiene copolymer	Polyethylene	
	Wood	Polypropylene	
	Hard rubber	Polydiphenyl propane carbonate	
	Acetate, Rayon	Polyimide (Kapton)	
	Polymethyl methacrylate (Lucite)	Polyethylene terephthalate	
	Polyvinyl alcohol	Polyvinyl Chloride (PVC)	
	(continued)	Polytrifluorochloroethylene	
		Polytetrafluoroethylene (Teflon)	

1.5 Van de Graaff Generator

Traditional triboelectric generator is a mechanical device that produces static electricity, or electricity at high voltage by contact charging. The most popular ones are the Wimshurst machine and Van de Graaff generator, which were invented in ~1880 and 1929, respectively. Both machines use the accumulated static charges generated by triboelectrification. A simple Van de Graaff generator consists of a belt of rubber (or a similar flexible dielectric material) running over two rollers of differing material, one of which is surrounded by a hollow metal sphere, as shown in Fig. 1.5 [17]. Two electrodes, (2) and (7), in the form of comb-shaped rows of sharp metal points, are positioned near the bottom of the lower roller and inside the sphere, over the upper roller. Comb (2) is connected to the sphere, and comb (7) to ground. The rubber of the belt will become negatively charged while the acrylic



**Fig. 1.5** The Van de Graaff generator and its working mechanism. Reproduced from Ref. [17]

glass of the upper roller will become positively charged. The belt carries away negative charge on its inner surface while the upper roller accumulates positive charge. Next, the strong electric field surrounding the positive upper roller (3) induces a very high electric field near the points of the nearby comb (2). At the points, the field becomes high enough to ionize air molecules, and the electrons are attracted to the outside of the belt while positive ions go to the comb. At the comb (2) they are neutralized by electrons that were on the comb, thus leaving the comb and the attached outer shell (1) with fewer net electrons. The excess positive charge is accumulated on the outer surface of the outer shell (1), leaving no field inside the shell. Electrostatic induction by this method continues, building up very large amounts of charge on the shell.

In the example, the lower roller (6) is metal, which picks negative charge off the inner surface of the belt. The lower comb (7) develops a high electric field at its points that also becomes large enough to ionize air molecules. In this case the electrons are attracted to the comb and positive air ions neutralize negative charge on the outer surface of the belt, or become attached to the belt. As the belt continues to move, a constant ‘charging current’ travels via the belt, and the sphere continues to accumulate positive charge until the rate that charge is being lost (through leakage and corona discharges) equals the charging current. The metal sphere (8) is connected to ground, as is the lower comb (7); electrons are drawn up from ground due to the attraction by the positive sphere, and when the electric field is large enough (see below) the air breaks down in the form of an electrical discharge spark (9). Since the material in the belt and rollers can be selected, the accumulated

charge on the hollow metal sphere can either be made positive (electron deficient) or negative (excess electrons).

Van de Graaff generator is a high voltage source, and there is no current unless there is a discharging. For a polished spherical electrode of 30 cm in diameter, it could be expected to develop a maximum voltage of about 450 kV.

## 1.6 Triboelectric Nanogenerators

Today's electronics is mostly associated with human activities for the purpose of health, safety and communication. The most abundant energy associated with a human is mechanical energy as a result of body motion. Recently, using the electrostatic charges created on the surfaces of two dissimilar materials when they are brought into physical contact, the contact induced triboelectric charges can generate a potential drop when the two surfaces are separated by mechanical force, which can drive electrons to flow between the two electrodes built on the top and bottom surfaces of the two materials. This is the first triboelectric nanogenerator (TENG) invented by Wang's group in 2012, aiming at harvesting small scale mechanical energy [18–20]. TENG has four basic modes as elaborated in details below.

### 1.6.1 *Vertical Contact-Separation Mode*

We use the simplest design of TENG as an example (Fig. 1.6a) [21, 22]. Two dissimilar dielectric films face with each other, and there are electrode being deposited on the top and the bottom surfaces of the stacked structure. A physical contact between the two dielectric films creates oppositely charged surfaces. Once the two surfaces are separated by a small gap under the lifting of an external force, a potential drop is created. If the two electrodes are electrically connected by a load, free electrons in one electrode would flow to the other electrode to build an opposite potential in order to balance the electrostatic field. Once the gap is closed, the triboelectric charge created potential disappears, the electrons flow back.

### 1.6.2 *Lateral Sliding Mode*

The structure to start with is the same as that for the vertical contact-separation mode. When two dielectric films are in contact, a relative sliding in parallel to the surface also creates triboelectric charges on the two surfaces (Fig. 1.6b) [23, 24]. A lateral polarization is thus introduced along the sliding direction, which drives the electrons on the top and bottom electrodes to flow in order to fully balance the field

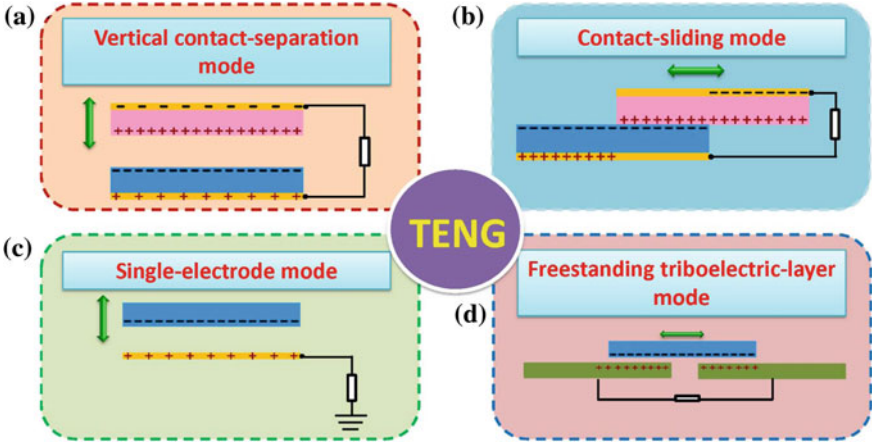


**Fig. 1.6** The four fundamental modes of triboelectric nanogenerators: **a** vertical contact-separation mode; **b** in-plane contact-sliding mode; **c** single-electrode mode; and **d** freestanding triboelectric-layer mode

created by the triboelectric charges. A periodic sliding apart and closing generates an AC output. This is the sliding mode TENG. The sliding can be a planar motion, a cylindrical rotation, or disc rotation. Related theoretical studies have been carried out for understanding the basic mode and grating structured TENG.

### 1.6.3 Single-Electrode Mode

The two modes introduced in Sects. 1.6.1 and 1.6.2 have two electrodes interconnected by a load. Such TENGs can freely move so that it can work for mobile cases. In some cases, the object that is part of the TENG cannot be electrically connected to the load because it is a mobile object, such as a human walking on a floor. In order to harvest energy from such a case, we introduced a single electrode TENG, in which the electrode on the bottom part of the TENG is grounded (Fig. 1.6c). If the size of the TENG is finite, an approaching or departing of the top object from the bottom one would change the local electrical field distribution, so that there are electron exchanges between the bottom electrode and the ground to maintain the potential change of the electrode. This energy harvesting strategy can be in both contact-separation mode [25] and contact-sliding mode [26, 27].

### 1.6.4 Freestanding Triboelectric-Layer Mode

In nature, a moving object is naturally charged due to its contact with air or other object, such as our shoes walking on floors that are usually charged. The charges

remain on surface for hours and the contact or friction is unnecessary within this period of time because the charge density reaches a maximum. If we make a pair of symmetric electrode underneath a dielectric layer and the size of the electrodes and the gap distance between the two are of the same order as the size of the moving object, the object's approaching to and/or departing from the electrodes create an asymmetric charge distribution in the media, which causes the electrons to flow between the two electrodes to balance the local potential distribution (Fig. 1.6d) [28]. The oscillation of the electrons between the pair electrodes produces power. The moving object does not have to be directly touch the top dielectric layer of the electrodes, so that, in rotation mode, a free rotation is possible without direct mechanical contact, so that the wearing of the surfaces can be drastically reduced. This is a good approach for extend the durability of the TENGs.

Based on the four modes illustrated above, we have fabricated various TENGs depending on specific applications. Figure 1.7 shows a collection of photographs of

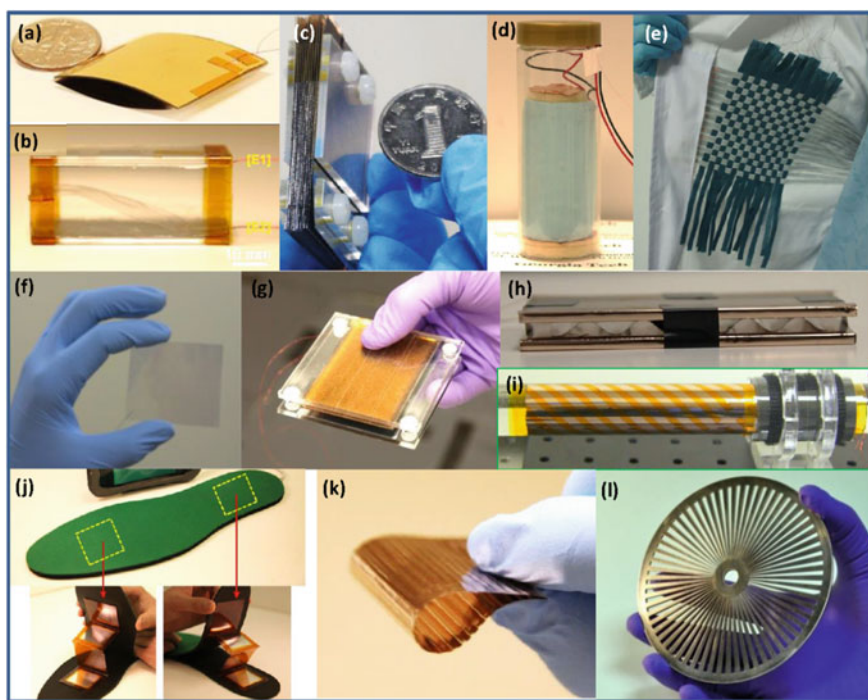


**Fig. 1.7** Typical photographs of some triboelectric nanogenerators fabricated for harvesting **a** finger tapping energy; **b** air-flow/wind energy; **c** relative in-plane sliding energy; **d** enclosed cage for harvesting oscillating/disturbing energy in water or mechanical vibration; **e** fabric for harvesting body motion energy; **f** transparent TENG for harvesting energy in touch pad; **g** foot/hand pressing energy; **h** water impact energy; **i** cylindrical rotation energy; **j** shoe insole for walking energy; **k** flexible grating structure for harvesting sliding energy; and **l** disc shape rotation energy. Reproduced with permission from Royal Society of Chemistry [32]

TENGs we have fabricated for harvesting various types of energy. These structures are the fundamental units for providing micro-scale power for small electronics, the assembly and integration of them can be the basis of harvesting mega-scale energy.

## 1.7 Perspectives

The discovery of triboelectric nanogenerator (TENG) is a major milestone in the field of converting mechanical energy into electricity for building self-powered systems. It offers a completely new paradigm for effectively harvesting mechanical energy using organic and inorganic materials. As of today, the area power density produced by a TENG has reached as high as  $500 \text{ W m}^{-2}$ , volume power density reaches  $15 \text{ MW m}^{-3}$ , and an instantaneous conversion efficiency of  $\sim 70\%$  has been demonstrated (Fig. 1.8) [29]. For low frequency agitation and if the energy generated by all the residual vibrations are acquired, a total energy conversion efficiency of up to  $85\%$  has been shown experimentally [30]. A standard for measuring the performance of a TENG has been established. The TENG can be applied to harvest all kinds of mechanical energies that are available but wasted in our daily life, such as human motion, walking, vibration, mechanical triggering, rotating tire, wind, flowing water and more [19, 20]. This is the first major area of applications of TENG as micro-/nano-scale power source (Fig. 1.9).

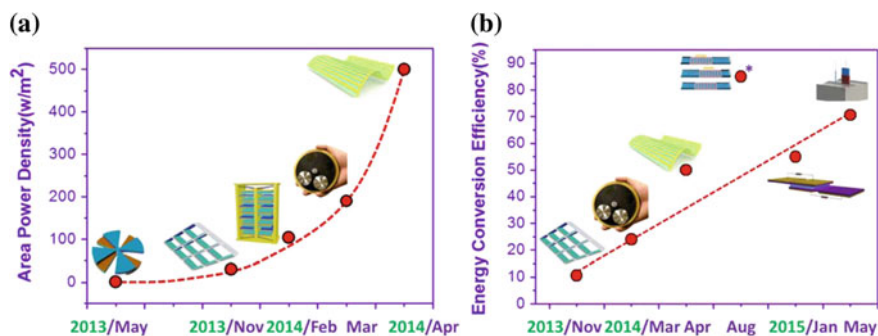


**Fig. 1.8** Summary on the progress in the performance of TENG made in the **a** area output power density and **b** energy conversion efficiency within the last 12 months. In May 2015, an instantaneous energy conversion efficiency of  $\sim 70\%$  has been demonstrated using liquid metal as a contact material. For low frequency agitation and if the energy generated by all the residual vibrations are acquired, a total energy conversion efficiency of up to  $85\%$  has been shown experimentally in 2014. \* Total energy conversion efficiency; the rest of data are instantaneous energy conversion efficiency. Reproduced with permission from Royal Society of Chemistry [20]



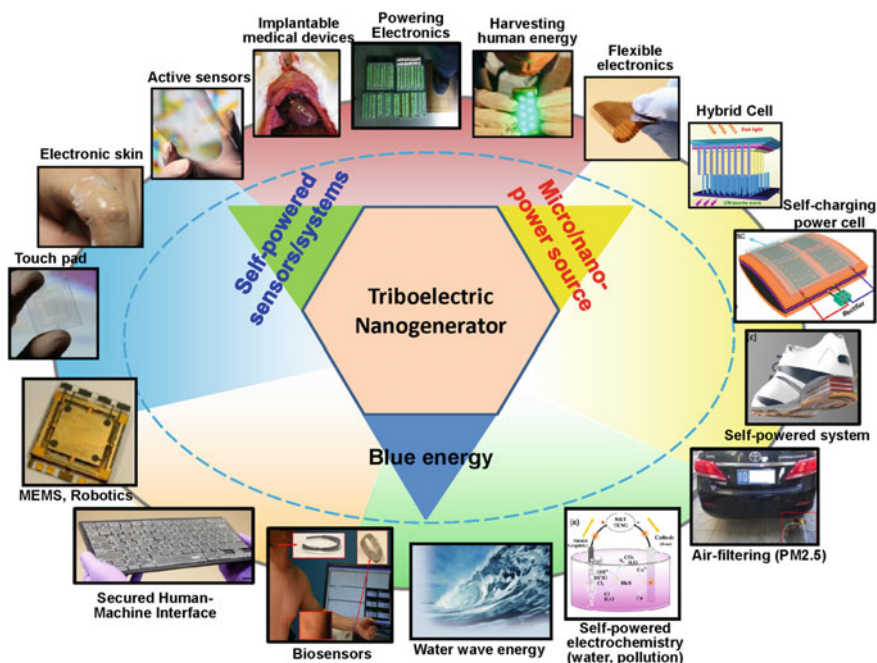


**Fig. 1.9** Summary on the three major field of applications of TENG in micro/nano-power source, self-powered sensors/systems (or active sensors) and mega-scale blue energy. The selected examples were from the research of Wang's group in the field of mobile/wearable electronics, internet of things, environmental science, medical sciences human-machine interfaces, infrastructure monitoring and security

Alternatively, a TENG can also be used as a self-powered sensor for actively detecting the static and dynamic processes arising from mechanical agitation using the voltage and current output signals of the TENG, respectively, with potential applications as mechanical sensors and for touch pad and smart skin technologies [31] (Fig. 1.9). Such sensor does not need an external power source, but creates electric signal itself in responding to the external triggering or stimulation.

Furthermore, by integrating TENGs into network structure, it has the potential to harvest water wave energy in ocean, which could be a new paradigm for mega-scale blue energy [32–34] (Fig. 1.9). TENG has the incompatible efficiency for harvesting low-frequency mechanical energy in comparison to traditional electromagnetic generator of equivalent volume, so that it has unique and killer applications for the exploration of ocean wave energy—*blue energy*, which has the potential of making a huge contribution to the sustainable energy for the world. Figure 1.10 shows a proposed technology development road map for nanogenerators and its commercial applications. Furthermore, TENG can serve as a

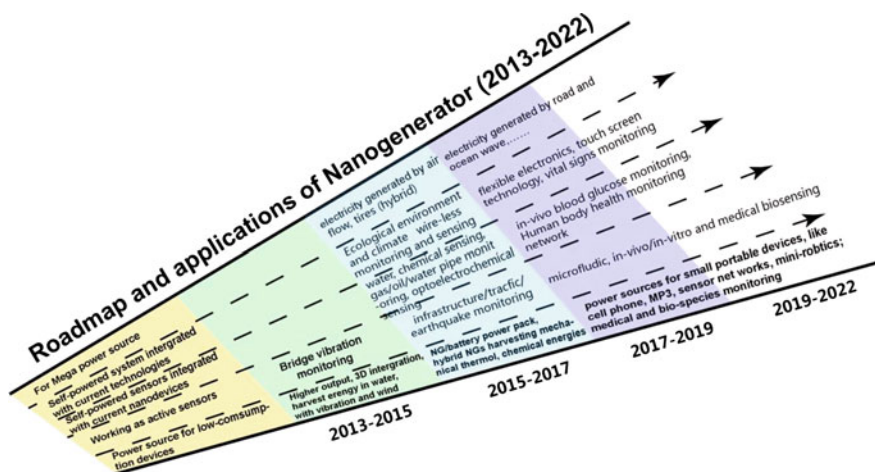


**Fig. 1.10** Proposed technology roadmap for nanogenerators (2012) by Wang. Reproduced with permission from Royal Society of Chemistry [32]

self-powered sensor for sensing mechanical triggering, pressure, muscle stretching and more, which may become commercially available sooner than energy harvesters.

## References

1. Z.L. Wang, J. Song, Piezoelectric nanogenerators based on zinc oxide nanowire arrays. *Science* **312**(5771), 242–246 (2006)
2. Z.L. Wang, Nanogenerators for self-powered devices and systems. Georgia Institute of Technology, SMARTech digital repository (2011). <http://hdl.handle.net/1853/39262>
3. Z.L. Wang, ZnO nanowire and nanobelt platform for nanotechnology. *Mater. Sci. and Eng. Rep.* **64**(3), 33–71 (2009)
4. Z.L. Wang, R. Yang, J. Zhou, Y. Qin, C. Xu, Y. Hu, S. Xu, Lateral nanowire/nanobelt based nanogenerators, piezotronics and piezo-phototronics. *Mater. Sci. and Eng. Rep.* **70**(3), 320–329 (2010)
5. Z.L. Wang, W. Wu, Nanotechnology-enabled energy harvesting for self-powered micro-/nanosystems. *Angew. Chem. Int. Ed.* **51**(47), 11700–11721 (2012)
6. J. Henniker, Triboelectricity in polymers. *Nature* **196**(474) (1962)
7. D. Davies, Charge generation on dielectric surfaces. *J. Phys. D Appl. Phys.* **2**(11), 1533 (1969)
8. R. Elsdon, F. Mitchell, Contact electrification of polymers. *J. Phys. D Appl. Phys.* **9**(10), 1445 (1976)
9. L.S. McCarty, G.M. Whitesides, Electrostatic charging due to separation of ions at interfaces: contact electrification of ionic electrets. *Angew. Chem. Int. Ed.* **47**(12), 2188–2207 (2008)
10. J.J. Cole, C.R. Barry, R.J. Knuesel, X. Wang, H.O. Jacobs, Nanocontact electrification: patterned surface charges affecting adhesion, transfer, and printing. *Langmuir* **27**(11), 7321–7329 (2011)
11. H.T. Baytekin, B. Baytekin, S. Soh, B.A. Grzybowski, Is water necessary for contact electrification? *Angew. Chem. Int. Ed.* **50**(30), 6766–6770 (2011)

12. H. Baytekin, A. Patashinski, M. Branicki, B. Baytekin, S. Soh, B.A. Grzybowski, The mosaic of surface charge in contact electrification. *Science* **333**(6040), 308–312 (2011)
13. Y.S. Zhou, Y. Liu, G. Zhu, Z.-H. Lin, C. Pan, Q. Jing, Z.L. Wang, In situ quantitative study of nanoscale triboelectrification and patterning. *Nano Lett.* **13**(6), 2771–2776 (2013)
14. Y.S. Zhou, S. Wang, Y. Yang, G. Zhu, S. Niu, Z.-H. Lin, Y. Liu, Z.L. Wang, Manipulating nanoscale contact electrification by an applied electric field. *Nano Lett.* **14**(3), 1567–1572 (2014)
15. J. Lowell, A. Rose-Innes, Contact electrification. *Adv. Phys.* **29**(6), 947–1023 (1980)
16. <http://owlsmag.wordpress.com/2010/01/20/a-natural-history-devin-corbin/>
17. [https://en.wikipedia.org/wiki/Van\\_de\\_Graaff\\_generator](https://en.wikipedia.org/wiki/Van_de_Graaff_generator)
18. F.-R. Fan, Z.-Q. Tian, Z.L. Wang, Flexible triboelectric generator. *Nano Energy* **1**(2), 328–334 (2012)
19. Z.L. Wang, Triboelectric nanogenerators as new energy technology for self-powered systems and as active mechanical and chemical sensors. *ACS Nano* **7**(11), 9533–9557 (2013)
20. Z.L. Wang, J. Chen, L. Lin, Progress in triboelectric nanogenerators as a new energy technology and self-powered sensors. *Energy Environ. Sci.* **8**(8), 2250–2282 (2015)
21. G. Zhu, C. Pan, W. Guo, C.-Y. Chen, Y. Zhou, R. Yu, Z.L. Wang, Triboelectric-generator-driven pulse electrodeposition for micropatterning. *Nano Lett.* **12**(9), 4960–4965 (2012)
22. S. Wang, L. Lin, Z.L. Wang, Nanoscale triboelectric-effect-enabled energy conversion for sustainably powering portable electronics. *Nano Lett.* **12**(12), 6339–6346 (2012)
23. S. Wang, L. Lin, Y. Xie, Q. Jing, S. Niu, Z.L. Wang, Sliding-triboelectric nanogenerators based on in-plane charge-separation mechanism. *Nano Lett.* **13**(5), 2226–2233 (2013)
24. G. Zhu, J. Chen, Y. Liu, P. Bai, Y.S. Zhou, Q. Jing, C. Pan, Z.L. Wang, Linear-grating triboelectric generator based on sliding electrification. *Nano Lett.* **13**(5), 2282–2289 (2013)
25. Y. Yang, Y.S. Zhou, H. Zhang, Y. Liu, S. Lee, Z.L. Wang, A single-electrode based triboelectric nanogenerator as self-powered tracking system. *Adv. Mater.* **25**(45), 6594–6601 (2013)
26. Y. Yang, H. Zhang, J. Chen, Q. Jing, Y.S. Zhou, X. Wen, Z.L. Wang, Single-electrode-based sliding triboelectric nanogenerator for self-powered displacement vector sensor system. *ACS Nano* **7**(8), 7342–7351 (2013)
27. S. Niu, Y. Liu, S. Wang, L. Lin, Y.S. Zhou, Y. Hu, Z.L. Wang, Theoretical investigation and structural optimization of single-electrode triboelectric nanogenerators. *Adv. Funct. Mater.* **24**(22), 3332–3340 (2014)
28. S. Wang, Y. Xie, S. Niu, L. Lin, Z.L. Wang, Freestanding triboelectric-layer-based nanogenerators for harvesting energy from a moving object or human motion in contact and non-contact modes. *Adv. Mater.* **26**(18), 2818–2824 (2014)
29. W. Tang, T. Jiang, F.R. Fan, A.F. Yu, C. Zhang, X. Cao, Z.L. Wang, Liquid—metal electrode for high-performance triboelectric nanogenerator at an instantaneous energy conversion efficiency of 70.6 %. *Adv. Funct. Mater.* (2015)
30. Y. Xie, S. Wang, S. Niu, L. Lin, Q. Jing, J. Yang, Z. Wu, Z.L. Wang, Grating-structured freestanding triboelectric-layer nanogenerator for harvesting mechanical energy at 85 % total conversion efficiency. *Adv. Mater.* **26**(38), 6599–6607 (2014)
31. S. Wang, L. Lin, Z.L. Wang, Triboelectric nanogenerators as self-powered active sensors. *Nano Energy* **11**, 436–462 (2015)
32. Z.L. Wang, Triboelectric nanogenerators as new energy technology and self-powered sensors —Principles, problems and perspectives. *Faraday Discuss.* **176**, 447–458 (2014)
33. J. Chen, J. Yang, Z. Li, X. Fan, Y. Zi, Q. Jing, H. Guo, Z. Wen, K.C. Pradel, S. Niu, Networks of triboelectric nanogenerators for harvesting water wave energy: a potential approach toward blue energy. *ACS Nano* **9**(3), 3324–3331 (2015)
34. X. Wang, S. Niu, Y. Yin, F. Yi, Z. You, Z.L. Wang, Triboelectric nanogenerator based on fully enclosed rolling spherical structure for harvesting low-frequency water wave energy. *Adv. Energy Mater.* **5**(24), (2015)

<http://www.springer.com/978-3-319-40038-9>

Triboelectric Nanogenerators

Wang, Z.; Lin, L.; Chen, J.; Niu, S.; Zi, Y.

2016, XXXIII, 517 p. 211 illus., 24 illus. in color.,

Hardcover

ISBN: 978-3-319-40038-9